Application of CO_2 Laser Heating Zone Drawing and Zone Annealing to Nylon 6 Fibers

AKIHIRO SUZUKI, MASAYOSHI ISHIHARA

Department of Applied Chemistry and Biotechnology, Faculty of Engineering, Yamanashi University, 4-3-11 Takeda, Kofu 400-8511 Japan

Received 29 March 2001; accepted 25 May 2001

ABSTRACT: Nlon 6 fibers were zone drawn and zone annealed by using a continuous wave carbon dioxide laser to develop their mechanical properties. A laser-heating zone drawing was carried out under a applied tension of 35.4 MPa at a power density of 9.65 $W \cdot cm^{-2}$, and then the zone-drawn fiber was annealed. A laser-heating zone annealing was carried out in two steps at a power density of 9.65 $W \cdot cm^{-2}$; the first step was carried out under 423 MPa and the second under 517 MPa. The treating temperature of the fiber heated by the CO_2 laser was measured by using an infrared thermographic camera equipped with a magnifying lens. The treating temperature at the zone drawing is 138°C, and those at the first and the second zone annealing are 121 and 125°C, respectively. The second laser-heated zone-annealed fiber has a birefringence of 65.2 $\times 10^{-3}$, a degree of crystallinity of 54%, and a storage modulus of 21 GPa at 25°C. Wide-angle X-ray diffraction patterns for the laser-heated zone-drawn and the zone-annealed fibers show (200) reflection and (002/202) doublet due to only an α form on the equator. The laser-heated zone-drawn fiber has a melting endotherm peaking at 216°C and a trace of shoulder on the higher temperature side of its peak, and the laser-heated zone-annealed fibers have a single melting endotherm peaking at 216°C. © 2002 John Wiley & Sons, Inc. J Appl Polym Sci 83: 1711–1716, 2002

Key words: nylon; fiber; laser; high performance polymers; drawing; annealing

INTRODUCTION

A carbon dioxide (CO_2) laser has been used in a laser cladding to improve surface wear and corrosion resistance properties of ceramic or metallic matrix composites and in a laser cutting of metallic coated sheet steels.[1–6] The CO_2 laser, however, was hardly applied to a drawing and annealing of polymers.[7,8]

We have so far applied a CO_2 laser-heating zone-drawing and zone-annealing method to poly(ethylene terephthalate) (PET) fiber.[9] This method was found to be improving the mechanical properties of the PET fiber. Unlike the laser cutting and coating carried out at a high power, the CO_2 laser used in the zone drawing and zone annealing was a continuous-wave carbon dioxide (CW CO_2) laser with a low laser power of about 1 W.

In this study, we present here the results pertaining to the mechanical properties and microstructure of the nylon 6 fibers zone drawn and zone annealed by the CW CO_2 laser.

Correspondence to: A. Suzuki (a-suzuki@ab11.yamanashi.ac.jp).

Contract grant sponsor: Grant-in-Aid for Scientific Research of Japan Society.

Journal of Applied Polymer Science, Vol. 83, 1711–1716 (2002)

DOI 10.1002/app.10094

EXPERIMENTAL

Material

The original material used in the present study was as-spun nylon 6 fibers supplied by Toray Ltd

and a commercial-grade fiber. The original fiber had a diameter of about 0.262 mm, the degree of crystallinity of 28%, and birefringence of 1.2×10^{-3}. The original fiber was found to be isotropic from a wide-angle X-ray diffraction photograph.

Apparatus for CW CO_2 Laser-Heating Method

A schematic diagram of the apparatus used for the CO_2 laser-heating zone drawing and zone annealing is given in Figure 1. The apparatus consists of a CW CO_2 laser emitter (PIN10S, ONIZCA glass Ltd.), a power meter with a thermal head, a tensile testing machine (Orientec Co. Ltd.) to achieve a downward movement of the fiber at 100 mm/min, an air cylinder used to raise and lower the thermal head, an infrared thermographic camera (TH3101MR, NEC San-ei Instruments, Ltd.) equipped with a magnifying lens, and a computer used to visualize data from the infrared thermographic camera. The CO_2 laser emitted light at 10.6 μm, and the laser beam was a 4.3-mm diameter spot. A beam power was measured by the power meter before the laser heating.

One end of the as-spun fiber was connected to a jaw equipped with crosshead of the tensile testing machine, while the other is attached to an arbitrary weight after passing through the two fixed pulleys. The laser beam was irradiated to the fiber, and can be absorbed fully by the fiber. The fiber was moved downward by moving the crosshead at a speed of 100 mm/min and drawn or annealed by irradiating the CW CO_2 laser ranging in power from 0.5 to 0.9 W.

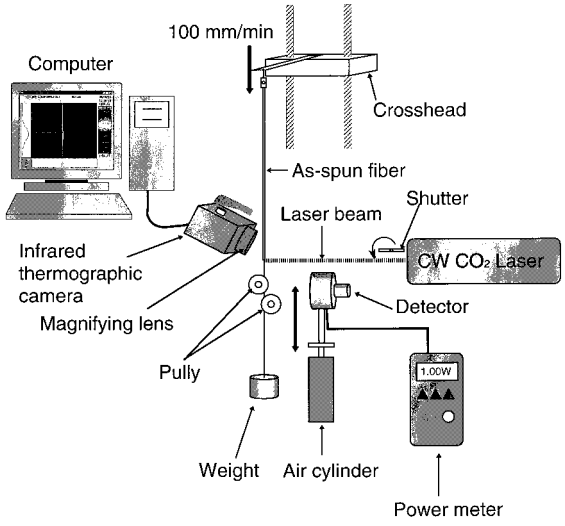

Figure 1 Scheme of apparatus used for laser heating zone drawing and laser heating zone annealing.

Measurement

The draw ratio was determined in the usual way, by measuring the displacement of ink marks placed 10 mm apart on the fiber before drawing. Birefringence was measured with a polarizing microscope equipped with a Berek compensator.

Density (ρ) was measured at 23°C by a flotation technique using a carbon tetrachloride and toluene mixture. The degree of crystallinity, expressed as a weight fraction (X_w), was obtained using the relation:

$$X_w = \{\rho_c(\rho - \rho_a)\}/\{\rho(\rho_c - \rho_a)\} \times 100 \qquad (1)$$

where ρ_c and ρ_a are densities of crystalline and amorphous phases, respectively. In this measurement, a value of 1.230 g/cm^3 was assumed for ρ_c,[10] and a value of 1.084 g/cm^3 was assumed for ρ_a.[11] The density of amorphous polymer was assumed to be constant, independent of treatments.

Equatorial wide-angle X-ray diffraction patterns for the fibers were obtained with a Rigaku X-ray generator and diffractometer equipped with a fiber specimen attachment. The X-ray unit was operated at 40 kV and 20 mA, and the radiation used was Ni-filtered CuK_α. Wide-angle X-ray diffraction photographs of the fibers were taken using a laue camera. The laue camera was attached to a Rigaku X-ray generator that was operated at 36 kV and 18 mA. The radiation used was Ni-filtered CuK_α. The sample-to-film distance was 40 mm. The fiber was exposed for 4 h to the X-ray beam from a pinhole collimator with a diameter of 0.4 mm.

Dynamic viscoelastic properties were measured at 110 Hz with a dynamic viscoelastometer Vibron DDV-II (Orientec Co. Ltd.). A 20-mm length of monofilament was needed between two jaws. Measurements were carried out over a temperature range of 25°C to about 200°C at an interval of 5°C. The average heating rate was 2°C/min.

RESULTS AND DISCUSSION

Optima Conditions for Laser Heating Zone Drawing and Laser Heating Zone Annealing

A significant improvement in the mechanical properties of crystalline polymers can be obtained

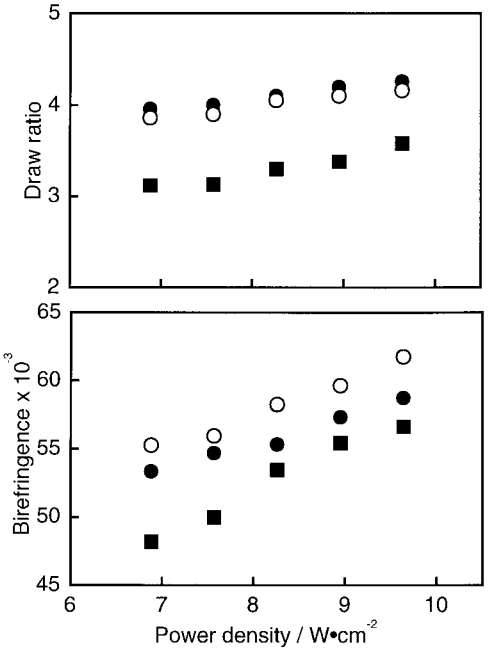

Figure 2 Changes in draw ratio and birefringence of the fibers zone drawn by laser heating at various power densities: (■) σ_a = 31.8 MPa, (○) σ_a = 35.4 MPa, (●) σ_a = 38.9 MPa.

by increase in fraction of taut tie chains. The increase of the tie chains would be promoted by the conversion of an original spherulitic lamellar structure into an extended microfibrillar form. The optimum drawing temperature to induce the a pronounced morphological change and the increase in overall molecular orientation lies between the glass transition and the melting point.[12] Furthermore, the evolution of crystallization is needed for the subsequent annealing. To achieve these objects, the laser heating zone drawing and the zone annealing were examined at powers varying from 0.5 to 0.9 W.

To determine the optimum condition of the laser heating zone drawing, the as-spun nylon 6 fiber was drawn under various conditions. A drawing speed used throughout the zone drawing was 100 mm/min. The optimum drawing condition was determined by measuring the draw ratio (λ) and the birefringence (Δn) of the drawn fibers.

Figure 2 shows the changes in the λ and the Δn of the fibers drawn under three different applied tensions (σ_a) with a power density (PD). The λ depends on the PD, and the σ_a, but the difference in the λ between the fibers drawn under 35.4 and 38.9 MPa is small. The Δn value increases with increasing the PD, but Δns at σ_a = 38.9 MPa are lower than those at σ_a = 35.4 MPa at each PD. The maximum value is given by the fiber drawn under 35.4 MPa at PD = 9.65 W · cm^{-2} and is 62 × 10^{-3}. The decrease in the Δn at the highest σ_a is attributable to molecular relaxation originated from chain rupture induced by an excessive loading. Consequently, the condition giving the maximum Δn was chosen as an optimum one for the laser heating zone drawing. Furthermore, though we attempted the zone drawing at the higher PD, the Δn could not be remarkably improved. The fiber zone drawn under the optimum condition will hereinafter abbreviated the LH-ZD fiber.

To optimize the condition of the laser heating zone annealing, the LH-ZD fibers were zone annealed under conditions of varying σ_as and PDs. The laser heating zone annealing was carried out in two steps, and an annealing speed used throughout the zone annealing was 100 mm/min. The optima conditions for the first and second zone annealing were also determined in the same way as in the case of the zone drawing. The condition giving the maximum Δn at each step was chosen as the optimum condition. The fibers obtained by the first and second zone annealing under the optima conditions are designated as the LH-ZA1 and LH-ZA2 fiber, respectively. The optima conditions for the laser heating zone drawing and zone annealing, together with the treating temperature measured using the infrared camera, are summarized in Table I. The microstructure and the dynamic viscoelastic properties of the fiber obtained under each optimum condition will be discussed below.

Relation between Treating Temperature and CO_2 Laser Power

In the laser-heating treating, it is impossible to measure the treating temperature of the thin fi-

Table I Optimum Conditions for the Laser Heating Zone Drawing, and Zone Annealing

Step	Applied Tension/ MPa	Treating Temperature/ °C	Power Density/ W · cm^{-2}
Zone drawing	35.4	138	
First zone annealing	423	121	9.65
Second zone annealing	517	125	

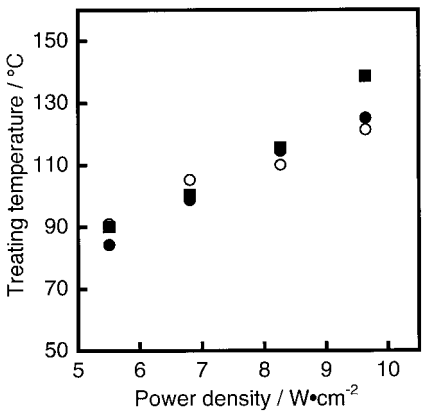

Figure 3 Relation between the treating temperature in the zone drawing and zone annealing and the power density: (■) zone drawing, (○) first zone annealing, (●) second zone annealing.

ber using a thermocuple because only the part that absorbed the laser beam becomes hot. Therefore, to measure the real treating temperature of the thin fiber, we used the infrared thermographic camera equipped with a magnifying lens. The infrared camera allows us to measure the real treating temperature and then has revealed the relation between the treating temperature and the laser power.

Figure 3 shows relation between the treating temperature in the laser heating zone drawing and zone annealing and the PD. The treating temperature is the maximum temperature in the thermography observed by the infrared camera. The treating temperature increases linearly with increasing the PD at each step. It became possible to measure the real treating temperature in the laser heating by the infrared camera with a magnifying lens.

Microstructure for the LH-ZD and LH-ZA Fibers

The λ, Δn, and X_w for the original, the LH-ZD, and the LH-ZA fibers are summarized in Table II, together with the Δn and X_w for the high-temperature zone-drawn (HT-ZD) nylon 6 fibers reported previously.[13] The high-temperature zone drawing was carried out in three steps, as shown in Table III. These values in both LH-ZD and HT-ZD fibers increase stepwise with the processing at each drawing, the LH-ZA2 fiber finally obtained has $\lambda = 5.2$, $\Delta n = 65.2 \times 10^{-3}$, and $X_w = 54\%$, and the HT-ZD3 fiber has $\Delta n = 58.3 \times 10^{-3}$ and $X_w = 54\%$. Although the X_w for the LH-ZD2 and HT-ZD3 fibers finally obtained is the same, there is a

Table II Draw Ratio, Birefringence (Δn), and Degree of Crystallinity (X_w) for the Original, the Laser-Heated Zone-Drawn (LH-ZD), Zone-Annealed (LH-ZA), and High-Temperature Zone-Drawn (HT-ZD) Fibers

Fiber	Draw Ratio	$\Delta n \times 10^3$	X_w/%
Original	—	1.16	28
LH-ZD	4.2	61.7	47
LH-ZA1	4.9	64.7	50
LH-ZA2	5.2	65.2	54
HT-ZD1	—	53.6	51
HT-ZD2	—	54.2	53
HT-ZD3	—	58.3	54

significant difference in Δn value. This difference may be attributed to the difference in degree of orientation of amorphous phase between the LH-ZD and HT-ZD fibers because the X_w of the two fibers is the same. The fact suggests that the laser heating is more effective in developing the orientation of amorphous phase when compared to the zone heating using a nichrom wire.

Figures 4 and 5 show the wide-angle X-ray diffraction photographs and equatorial patterns for the LH-ZD and the LH-ZA fibers. There are (200) reflection and (002/202) doublet due to an α form[14] on the equator, but no (200) reflection due to a γ form[15] is observed. It will be noted from Figures 4 and 5 that the morphology of crystallites existing in these fibers is only the α form, and that extremely high levels of crystalline orientation are obtained in the LH-ZA fibers.

Figure 6 shows DSC thermograms of the original, the LH-ZD, and the LH-ZA fibers. The original fiber shows a broad melting endotherm peaking at 219°C. The melting peaks can be attributed to melting of a folded chain crystal (FCC) existed

Table III Optimum Conditions for the High-Temperature Zone Drawing

Step	Applied Tension/ MPa	Treating Temperature/ °C
First high-temperature zone drawing	19.6	
Second high-temperature zone drawing	98.0	210
Third high-temperature zone drawing	127	

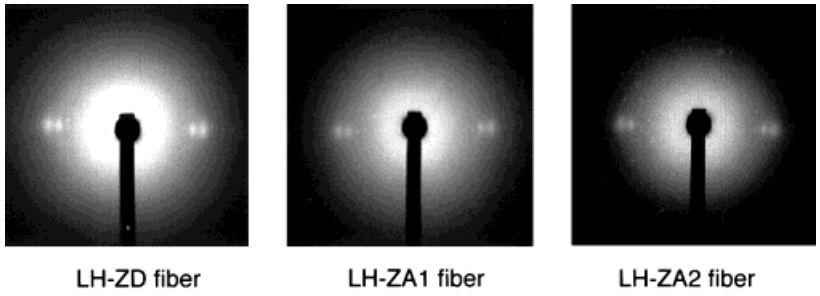

Figure 4 Wide-angle X-ray diffraction photographs of the LH-ZD, LH-ZA1, and LH-ZA2 fibers.

in the original fiber and/or to melting of the crystals recrystallized during the DSC measurements.[16,17] The LH-ZD fiber has a melting endotherm peaking at 216°C and the trace of shoulder on the higher temperature side of its peak, and the trace is observed at the same temperature as that at the higher melting peak of the original fiber. The appearance of a low-temperature melting peak is attributable to the morphological transformation of crystallite; the chain-folded crystalline structure in the original fiber changes partially into a fringed-micelle one with an unfolding of the chains. Elenga et al.[18] suggested from the standpoint of kinetics that the low-temperature melting peak was ascribed to the fringed-micelle crystals built up by chain unfolding, and the high-temperature one corresponds to the untransformed fraction of the lamellar crystals that undergo reorganization during the heating scan.

The LH-ZA fibers have only a single melting endotherm peaking at 216°C. The appearance of the single melting peak supposes that the FCC remained in the LH-ZD fiber change into the fringed-micelle crystals during the first laser-heating treatment, and that the recrystallization of the crystals induced by the zone drawing does not occur during the DSC scan.

Dynamic Viscoelastic Properties

Figure 7 shows the temperature dependence of storage modulus (E') and loss tangent (tan δ) for the original, the LH-ZD, and the LH-ZA fibers. The E' values over a wide temperature range increase progressively with the processing. Finally, the E' value of the LH-ZA2 fiber reaches 22 GPa at 25°C. The HT-ZD3 nylon 6 fiber reported previously[13] had 12 GPa at 25°C. The significant difference in the E' between the LH-ZA2 fiber and the HT-ZD3 fiber may be attributed to the difference in the orientation of amorphous phase between the two fibers. No significant decrease in E' due to an α relaxation described below is ob-

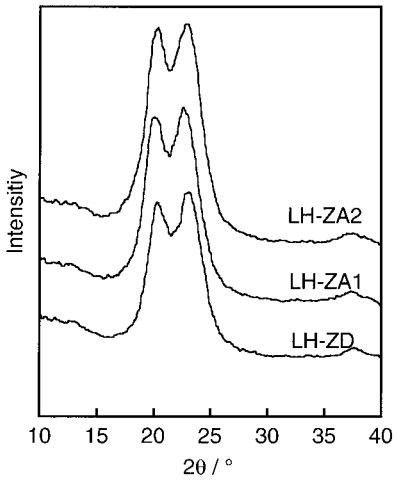

Figure 5 Equatorial wide-angle X-ray diffraction patterns of the LH-ZD, LH-ZA1, and LH-ZA2 fibers.

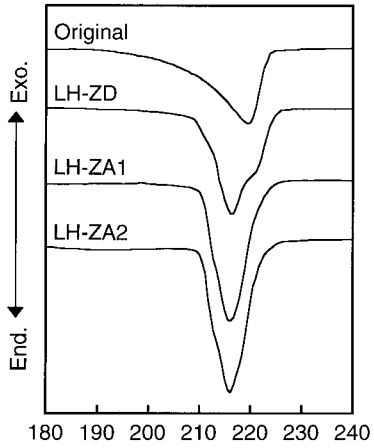

Figure 6 DSC curves of the original, LH-ZD, LH-ZA1, and LH-ZA2 fibers.

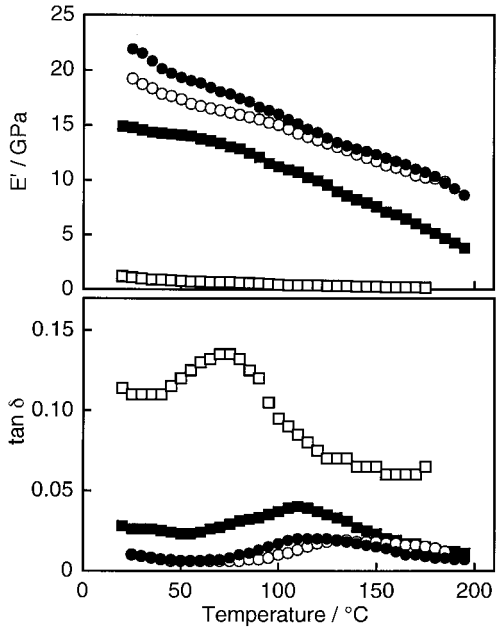

Figure 7 Temperature dependence of storage modulus (E') and loss tangent (tan δ) for the original fiber, HL-ZD, LH-ZA1, and LH-ZA2 fibers: (□) original, (■)LH-ZD, (○) LH-ZA1, (●) LH-ZA2.

served, the E' values of all the fibers decrease monotonously with increasing temperature.

In the temperature dependence of tan δ, α relaxation peaks are observed in the temperature range of 70 to 130°C. The peaks originate with a rupture of interchain hydrogen bonding due to the increase of motions of chain segments in the amorphous regions.[19,20] The α peak shifts to a higher temperature, decreases in its peak height, and becomes much broader with processing. The changes in position and in profile of the α peak with the processing point out that the molecular mobility in the amorphous regions is restricted by the surrounding crystallites.

CONCLUSIONS

The laser heating zone drawing and laser heating zone annealing method has been applied to the as-spun nylon 6 fibers to improve their mechanical properties. The CO_2 laser heating was found to be effective in producing the high-performance nylon 6 fibers.

The infrared camera allows us to measure the treating temperature of the fiber heated by the CO_2 laser. The temperature measurement using the infrared camera revealed the treating temperature in the laser heating zone drawing and zone annealing.

We are going to further study the effect of CO_2 laser on the molecular orientation and crystallization in the drawing and annealing for the nylon 6 fiber.

We acknowledge the financial support of the Grant-in-Aid for Scientific Research (C) of Japan Society for the Promotion of Science. We are grateful to Toray Ltd. for supplying nylon 6 fibers to us.

REFERENCES

1. Zergioti, I.; Hatziapostolou, A.; Hontzopoulos, E.; Zervaki, A.; Haidemenopoulos, G. N. Thin Solid Films 1995, 271, 96.
2. Wang, J.; Wong, W. C. K. J Mater Process Technol 1999, 95, 164.
3. Hopfe, V.; Jäckel, R.; Schönfeld, K. Appl Surf Sci 1996, 106, 60.
4. Paiva, P., Madelino, F.; Conde, O. J Lumin 1999, 80, 141.
5. Panzner, M.; Wiedemann, G.; Henneberg, K.; Fischer, R.; Wittke, Th.; Dietsch, R. Appl Surf Sci 1998, 127–129, 787.
6. Hidouci, A.; Pelletier, J. M.; Ducoin, F.; Dezert, D.; Guerjouma, R. El. Surf Coat Technol 2000, 123, 17.
7. Dadsetan, M.; Mirzadeh, H.; Shari, N. Radiat Phys Chem 1999, 56, 597.
8. Scarparo, M. A. F.; Chen, Q. J.; Miller, A. S.; Li, C. J.; Leary, H.; Allen, S. D. Appl Surf Sci 1996, 106, 275.
9. Suzuki, A.; Mochiduki, N. J Appl Polym Sci 2001, 82, 2775.
10. Holmes, D. R.; Bunn, C. W.; Smith, D. J. J Polym Sci 1955, 17, 159.
11. Roldan, L. G.; Kaufman, G. S. J Polym Sci Part B 1963, 1, 603.
12. Taylor, W. N., Jr.; Clark, E. S. Polym Eng Sci 1978, 18, 518.
13. Kunugi, T.; Suzuki, A.; Kubota, E. Kobunshi Ronbunsyu 1992, 49, 161.
14. Holmes, D. R.; Bunn, C. W.; Smith, D. J. J Polym Sci 1955, 17, 159.
15. Richardson, A.; Ward, I. M. J Polym Sci 1981, 19, 1549.
16. Pecorini, T. J.; Hertzberg, R. W. Polymer 1993, 34, 5053.
17. Quintanilla, L.; Rodríguez-Cabello, J. C.; Pastor, J. M. Polymer 1994, 35, 2321.
18. Elenga, R.; Seguela, R.; Rietsch, F. Polymer 1991, 32, 1975.
19. Papir, Y. S.; Kapur, S.; Rogers, C. E.; Baer, E. J Polym Sci 1972, 10, 1305.
20. Ning, X.; Ishida, H. J Polym Sci Part B 1991, 29, 1479.